JB Accepted Manuscript Posted Online 16 October 2017
J. Bacteriol. doi:10.1128/JB.00536-17
Copyright © 2017 American Society for Microbiology. All Rights Reserved.

Accepted Manuscript Posted Online
Journal of Bacteriology
JB
Journal of Bacteriology

Downloaded from http://jb.asm.org/ on October 20, 2017 by UC London Library Services

A single-cell view of the BtsSR/YpdAB pyruvate sensing network in *Escherichia coli* and its biological relevance

Cláudia Vilhena,[a] Eugen Kaganovitch,[b] Jae Yen Shin,[a*] Alexander Grünberger,[b] Stefan Behr,[a*] Ivica Kristoficova,[a] Sophie Brameyer,[a*] Dietrich Kohlheyer,[b,c] Kirsten Jung,[a]#

Munich Center for Integrated Protein Science (CIPSM) at the Department of Microbiology, Ludwig-Maximilians-Universität München, Martinsried, Germany[a]; Institute for Bio- and Geosciences, IBG-1: Biotechnology, Forschungszentrum Jülich GmbH, Jülich, Germany[b], RWTH Aachen University–Microscale Bioengineering (AVT.MSB) 52074 Aachen, Germany[c]

Running Head: Phenotypic heterogeneity in *E. coli*

#Address correspondence to Kirsten Jung, jung@lmu.de

[*]Present address: Alexander Grünberger, Multiscale Bioengineering, Bielefeld University, Universitätsstraße 25, 33615 Bielefeld; Stefan Behr, Roche Diagnostics GmbH, Nonnenwald 2 82377 Penzberg; Jae Yen Shin, MPI of Biochemistry, Am Klopferspitz 18 82152 Martinsried; Sophie Brameyer, University College London, Gower Street, WC1E 6EA London.

Accepted Manuscript Posted Online

ABSTRACT

Fluctuating environments and individual physiological diversity force bacteria to constantly adapt and optimize the uptake of substrates. Here we focus on two very similar two-component systems (TCSs) of *Escherichia coli* belonging to the LytS/LytTR family, BtsS/BtsR (formerly YehU/YehT) and YpdA/YpdB. Both TCSs respond to extracellular pyruvate, albeit with different affinity, typically during post-exponential growth, and each system regulates expression of a single transporter gene, *yjiY* and *yhjX*, respectively. To obtain insights into the biological significance of these TCSs, we analyzed the activation of the target promoters at the single-cell level. We found unimodal cell-to-cell variability; however, the degree of variance was strongly influenced by the available nutrients and differed between the two TCSs. We hypothesized that activation of either of the TCSs helps individual cells to replenish carbon resources. To test this hypothesis, we compared wild-type cells with the *btsSR ypdAB* mutant under two metabolically modulated conditions, protein overproduction and persister formation. While all wild-type cells were able to overproduce GFP, about half of the *btsSRypdAB* population was unable to overexpress GFP. Moreover, the percentage of persister cells, which tolerate antibiotic stress, was significantly lower in the wild-type than in the *btsSRypdAB* population. Hence, we suggest that the BtsS/BtsR and YpdA/YpdB network contributes to a balancing of the physiological state of all cells within a population.

IMPORTANCE Histidine kinase/response regulator (HK/RR) systems enable bacteria to respond to environmental and physiological fluctuations. *E. coli* and other members of the *Enterobacteriaceae* possess two similar LytS/LytTR-type HK/RRs, BtsS/BtsR (formerly YehU/YehT) and YpdA/YpdB, which form a functional network. Both systems are activated in

Journal of Bacteriology JB Journal of Bacteriology

Downloaded from http://jb.asm.org/ on October 20, 2017 by UC London Library Services

Accepted Manuscript Posted Online

response to external pyruvate, typically when cells face overflow metabolism during post-exponential growth. Single-cell analysis of the activation of their respective target genes *yjiY* and *yhjX* revealed cell-to-cell variability, and the range of variation was strongly influenced by externally available nutrients. Based on the phenotypic characterization of a *btsSRypdAB* mutant in comparison to the parental strain, we suggest that this TCS network supports an optimization of the physiological state of the individuals within the population.

Downloaded from http://jb.asm.org/ on October 20, 2017 by UC London Library Services

Journal of Bacteriology JB Journal of Bacteriology

Accepted Manuscript Posted Online

Journal of Bacteriology

JB

Journal of Bacteriology

Downloaded from http://jb.asm.org/ on October 20, 2017 by UC London Library Services

INTRODUCTION

Typical two-component systems (TCSs) consist of a membrane-bound histidine kinase (HK) which perceives a stimulus, and a cytoplasmic response regulator (RR) which triggers an appropriate response (1, 2). *Escherichia coli* contains 30 TCSs in all. Members of the LytS/LytTR family make up one prominent class of TCSs, representatives of which are found in many microorganisms. Examples include AgrC/AgrA from *Staphylococcus aureus*, which is involved in the transition from the persistent, avirulent state to the virulent phenotype (3), while FsrC/FsrA from *Enterococcus faecalis* is responsible for the production of virulence-related proteases (4) and VirS/VirR from *Clostridium perfringens* induces the synthesis of exotoxins and collagenase (5, 6). In our laboratory, we are studying the only two known members of the LytS/LytTR family in *E. coli*: BtsS/BtsR (previously YehU/YehT) and YpdA/YpdB (7–10). These two TCSs not only share the same domain structure, they also display over 30% identity at the amino acid sequence level (9). BtsS/BtsR activation leads to the expression of *yjiY*, YpdA/YpdB activation results in *yhjX* expression (**Fig. 1**). Both target genes code for transporters, which belong to different transporter families: YjiY is a member of the CstA family, and YhjX has been assigned to the oxalate/formate antiporter (OFA) family (7, 8, 11). In addition, the cyclic AMP (cAMP) receptor protein (CRP) complex (CRP-cAMP) up-regulates *yjiY* at the transcriptional level (7), while the carbon storage regulator A (CsrA) up-regulates *yhjX* and down-regulates *yjiY* at the post-transcriptional level.

In previous studies we found functional interconnectivity of the two TCSs (9). Deletion of either component of the TCS or its target gene influences the level of expression of the target gene regulated by the other TCS and vice versa (9). In addition, in vivo protein-protein interaction assays suggested that the two systems form a single, large signalling unit (**Fig. 1**). Moreover, when *E. coli* is grown in LB medium, both systems are activated at the onset of the

Accepted Manuscript Posted Online

Journal of Bacteriology

JB

Journal of Bacteriology

Downloaded from http://jb.asm.org/ on October 20, 2017 by UC London Library Services

post-exponential growth phase (9). A more refined study revealed that the BtsS/BtsR system is activated in the presence of extracellular pyruvate (at a threshold concentration of 50 µM) under nutrient-depleted conditions (10). Biochemical studies confirmed that BtsS is a high-affinity pyruvate receptor (K_d 58.6 µM) (10). Recently, the corresponding YjiY transporter was characterized as a high-affinity pyruvate/H^+ symporter (12). The YpdA/YpdB system also responds to extracellular pyruvate, albeit at a higher threshold concentration of 600 µM (8).

The biological significance of the BtsS/BtsR and YpdA/YpdB network is still unclear. To explore this issue, we determined the activation states of the two systems at the single-cell level in *E. coli* populations. Using separate fluorescence reporter strains for each system, we found a correlation between the available nutrient resources and the degree of heterogeneity in the transcriptional responses of the target gene promoters in individual cells. Based on this finding and further phenotypic analyses, we suggest that the BtsS/BtsR and YdpA/YpdB systems play a role in optimization of the physiological status of the individual cells within the population.

Accepted Manuscript Posted Online

Journal of Bacteriology

JB

Journal of Bacteriology

Downloaded from http://jb.asm.org/ on October 20, 2017 by UC London Library Services

RESULTS

Heterogeneous activation of P_{yhjX}-*gfp* and P_{yjiY}-*gfp*. For the BtsS/BtsR and YpdA/YpdB systems, population-based studies have shown that the promoters of their respective target genes, *yjiY* and *yhjX*, are activated in cells which face nutrient limitation and sense the presence of external pyruvate (9, 10). Since both systems are linked to form a network, we analyzed the activation of these two promoters at the single-cell level. We constructed fluorescent reporter strains by fusing the promoter regions of *yhjX* and *yjiY* to *gfp* and introduced each fusion separately into the genome of *E. coli* MG1655 via single homologous recombination at the native locus. By using this strategy the regulatory inputs to the native promoters of *yjiY* and *yhjX* were maintained (9), as the promoter fused to *gfp* is inserted upstream of the original one (13). The fluorescence intensity of GFP was used to quantify the activity of the two promoters, thus allowing us to study the transcriptional activation of *yjiY* and *yhjX* in single cells. The growth rates in LB medium of strains containing a chromosomal copy of either promoter fusion (from now on referred to as P_{yhjX}-*gfp* and P_{yjiY}-*gfp*) were similar to that of the MG1655 wild-type strain (**Fig. S1**).

From population studies it is known that in cells grown in LB medium, which is rich in amino acids and leads to overflow of pyruvate, both promoters are activated at the onset of the post-exponential growth phase (9). Hence, as expected, at the single-cell level neither P_{yhjX}-*gfp* nor P_{yjiY}-*gfp* showed any activity during the exponential growth phase (**Fig. 2A, 2C,** before activation) in LB medium. However, when cells reached the end of the exponential growth phase, we observed activation of the *yhjX* promoter, as indicated by a shift of the distribution of fluorescence intensities to higher levels (**Fig. 2A, 2B,** after activation) in the majority of the population, albeit with a high degree of cell-to-cell variability as seen in the width of the

Accepted Manuscript Posted Online

Journal of Bacteriology

JB

Journal of Bacteriology

Downloaded from http://jb.asm.org/ on October 20, 2017 by UC London Library Services

Gaussian distribution [noise value (standard deviation divided by the mean) 0.27]. Less than 4% of the population was found to be non-fluorescent and therefore did not respond (the threshold of activation is marked by the dashed line in **Fig. 2B**). To differentiate these cells from dead cells, we stained cells with propidium iodide and found that dead cells made up only 0.4% of the population (data not shown).

Cells of the P_{yjiY}-*gfp* strain cultivated in LB medium also showed heterogeneous activation upon entry into the post-exponential growth phase. These strains exhibited an even higher noise value of 0.52 and a higher percentage of non-responding cells (9%) (**Fig. 2D**) (the percentage of dead cells was determined to be 0.6%).

To determine the basal noise level of a promoter in cells at this growth phase, we performed a control experiment, in which *gfp* expression is controlled by a synthetic vegetative promoter (pXGSF, see **Table 1** for details). Cells harboring the vector pXGSF activate this promoter at the post-exponential growth phase (R. Hengge, personal information). In this experiment the promoter was activated in all the cells and the variability was lower (0.13) than that observed for either P_{yjiY}-*gfp* or P_{yhjX}-*gfp* (data not shown). Taken together, these results indicate a heterogeneous, almost unimodal pattern of transcriptional activation for each of the two target genes of the BtsS/BtsR and YpdA/YpdB systems at the end of the exponential phase, when cells are grown in LB medium.

The degree of heterogeneity of P_{yhjX}-*gfp* activation depends on the external pyruvate concentration. Although the exact nature of the primary stimulus for the YpdA/YpdB system remains elusive, we know from previous studies that P_{yhjX} is activated in cells which are exposed to extracellular pyruvate concentrations higher than 0.6 mM (9). Aiming to further explore the single-cell behavior of this promoter activity, we analyzed the pyruvate dependence of the

Accepted Manuscript Posted Online

Journal of Bacteriology

JB

Journal of Bacteriology

Downloaded from http://jb.asm.org/ on October 20, 2017 by UC London Library Services

142 activation of YpdA/YpdB by determining the fluorescence intensities of P_{yhjX}-*gfp* reporter cells
143 cultivated in M9 minimal medium supplemented with increasing concentrations of pyruvate
144 (succinate was added to keep the total carbon concentration constant at 20 mM) (**Fig. 3**). As
145 expected, a pyruvate concentration below the threshold (0.3 mM) failed to activate the
146 YpdA/YpdB system in single cells. At pyruvate concentrations above the threshold, all cells in
147 the population homogenously activate the *yhjX* promoter. The presence of 0.6 mM pyruvate in the
148 medium generated a low, but detectable P_{yhjX}-*gfp* signal in the cells and, the presence of 1 mM
149 pyruvate shifted the expression level towards higher values. Interestingly, the response was
150 markedly less heterogeneous (noise value of 0.18) in cells grown under these conditions than in
151 the cells grown in LB medium (noise value of 0.27). Further increases in the external pyruvate
152 concentration (2 mM and 10 mM) boosted the signal intensities, while the variability further
153 decreased (to 0.09 and 0.07, respectively) (**Fig. 3**). These results reveal a correlation between
154 external pyruvate availability and P_{yhjX}-*gfp* activation.
155
156 **The degree of heterogeneity in P_{yjiY}-*gfp* activation is influenced both by the external**
157 **pyruvate level and the metabolic state of the cells**. As previously described, growth of cells in
158 M9 minimal medium with pyruvate as sole carbon source (20 mM) is not sufficient to activate
159 the P_{yjiY} promoter, because both extracellular pyruvate and nutrient limitation are needed to
160 trigger BtsS/BtsR activation (10).Therefore, our reporter strain had first to be exposed to nutrient
161 limitation (growth in 0.1x LB medium for 1h) before pyruvate was added. Experimentally, *E. coli*
162 MG1655 P_{yjiY}-*gfp* was first grown in 0.1x LB medium for 1 h. Under these conditions, no
163 activation of P_{yjiY}-*gfp* was detected (data not shown), in accordance with our previous studies
164 (10). Pyruvate was then added to the cell culture at a final concentration of 20 mM, and cells
165 were analyzed by fluorescence microscopy at various time points. Cells responded within 70 min

Accepted Manuscript Posted Online

Journal of Bacteriology

JB

Journal of Bacteriology

Downloaded from http://jb.asm.org/ on October 20, 2017 by UC London Library Services

and exhibited a higher average *gfp* intensity than cells grown in LB medium, which confirmed the strong response of the BtsS/BtsR system to pyruvate after exposure of cells to nutrient limitation (**Fig. 4A**). Remarkably, in this case activation of P_{yjiY}-*gfp* remained heterogeneous (noise value of 0.27) in spite of the abundance of pyruvate. Subsequently, we tested five different pyruvate concentrations to assess the pyruvate concentration dependence of BtsS/BtsR activation (**Fig. 4B**). Below the threshold of 50 µM (0.01 mM) to which BtsS/BtsR responds, there was no detectable P_{yjiY}-*gfp* signal. As expected, only a few cells produced a weak GFP signal in an environment containing 0.05 mM pyruvate. Starting at a concentration of 0.1 mM pyruvate, P_{yjiY} activation was found in all cells, but with a high degree of cell-to-cell variability (noise value 0.27). At higher pyruvate concentrations, the signal intensity increased, but the noise values were unchanged. The broad Gaussian distribution found at 1 mM pyruvate resembled the profile found for cells at 20 mM pyruvate (**Fig. 4A**). A t-test was performed on the mean values of the two distributions and the P value was determined with 0.88. This value revealed that there is no significant difference between the cellular response at 1 and 20 mM pyruvate. These results confirmed at the single-cell level that BtsS/BtsR-mediated activation of P_{yjiY}-*gfp* is not only dependent on the pyruvate concentration, but is also influenced by internal nutrient limitation.

Cellular physiology in the post-exponential growth phase. We have shown thus far that transcriptional activation of both target genes of the BtsS/BtsR and YpdA/YpdB network occurs heterogeneously. Furthermore, their activation is influenced by the availability of external pyruvate, albeit with different thresholds.

In light of the fact that the two systems are activated in the post-exponential growth phase in LB medium, we decided to explore the impact of the BstS/BtsR and YpdA/YpdB systems on the overall physiological state of *E. coli* during this growth phase. In order to do so, we

Accepted Manuscript Posted Online

Journal of Bacteriology

JB

Journal of Bacteriology

Downloaded from http://jb.asm.org/ on October 20, 2017 by UC London Library Services

190 investigated individual cells of both *E. coli* MG1655 (the wild type, WT) in comparison with a
191 strain lacking both systems – MG1655 Δ*btsSbtsR* Δ*ypdAypdB* (abbreviated *btsSRypdAB* mutant).
192 Fast-growing cells express high levels of 16S RNA from the *rrnB* P1 promoter (14). Cells
193 with an inactive *rrnB* P1 promoter are likely to be dormant, antibiotic-tolerant persisters (14, 15).
194 Recently, the strength of *rrnB* P1 promoter activation was shown to correlate with intracellular
195 ATP levels. (16). We therefore fused the ribosomal *rrnB* P1 promoter to *gfp* as previously
196 described (14) and integrated this construct into the genomes of the two strains as a marker for
197 their physiological states.
198 As expected, *E. coli* MG1655 WT *rrnB* P1-*gfp* showed a Gaussian distribution of GFP
199 signal intensities, with a mean fluorescence value of 510 AU, and noise level of 0.16 (**Fig. 5**). In
200 contrast, the mutant *bstSRypdAB rrnB* P1-*gfp* had a lower overall *rrnB* P1-*gfp* activity (average
201 fluorescence intensity of 398 AU), which indicates a lower rate of ribosome synthesis within the
202 population. Most strikingly, a bistable distribution of the signal was observed. These results
203 suggest that, in the absence of both systems, the population differentiates into two
204 subpopulations, one with a normal and another with a reduced ribosome synthesis rate.
205
206
207 **The BtsSR/YpdAB network promotes protein overproduction.** To test the idea that
208 BtsS/BtsR and YpdA/YpdB systems together act to optimize the physiological state of cells
209 within the population, we set out to metabolically challenge the *bstSRypdAB* mutant and compare
210 its response to that of the parental *E. coli* MG1655 WT strain. Interestingly, *E. coli* C41 (DE3),
211 also known as the Walker strain, has been optimized for maximal overproduction of membrane
212 and globular proteins (17). Subsequently, the genome of this strain was sequenced and, among
213 other mutations, a point mutation in *btsS* was found that led to constitutive expression of *yjiY*

Accepted Manuscript Posted Online

Journal of Bacteriology

JB

Journal of Bacteriology

Downloaded from http://jb.asm.org/ on October 20, 2017 by UC London Library Services

(18). Based on these data, we hypothesized that the BtsS/BtsR and YpdA/YpdB systems might help cells to cope with the metabolic burden of protein overproduction.

In order to test this hypothesis, both strains (WT and the *bstSRypdAB* mutant) were transformed with the overexpression vector pBAD24-*gfp*, which carries *gfp* under the control of an arabinose-inducible promoter. Before induction with arabinose, fluorescence microscopy of single WT and *btsSRypdAB* mutant cells showed no apparent GFP signals and flow cytometry confirmed that the maximal fluorescence intensity of green cells (about 750 AU) was low (**Fig. 6A, 6C**), indicating little or no GFP expression. One hour after induction with 0.2 % (wt/vol) arabinose, cells of the WT population were producing GFP, which was clearly detected as an increase in the maximum fluorescence observed by flow cytometry (to about 1,100 AU). This result was corroborated by the detection of labeled single cells with fluorescence microscopy (**Fig. 6B**). In contrast, flow cytometric analysis of the mutant under inducing conditions detected two peaks - one at 1,100 AU as in the WT and a second at 750 AU. The accompanying micrographs revealed the presence of fluorescent and non-fluorescent cells (**Fig. 6D**). Therefore, the low-intensity peak in the flow cytometer represents cells that are unable to produce GFP in large amounts. The C41 (DE3) strain was also tested and was found to be capable of a homogeneously high protein overproduction, as expected (data not shown).

We also tested the overproduction of (i) GFP under the control of the IPTG-inducible *lac* promoter (pCOLA-P_{lac}-*gfp*), (ii) the periplasmic protein DppA fused to the Tat translocation sequence (19), under the control of the arabinose promoter (pBAD24-RR-*gfp-dppA*), and (iii) the membrane protein LysP fused to a different fluorophore, under the control of an arabinose-inducible promoter (pBAD33-*lysP-mcherry*) (**Table S1**). The results obtained for the IPTG-inducible GFP reporter were similar to those for the arabinose-controlled system. The

Accepted Manuscript Posted Online

Journal of Bacteriology

JB

Journal of Bacteriology

Downloaded from http://jb.asm.org/ on October 20, 2017 by UC London Library Services

237 *btsSRypdAB* mutant was hardly able to overproduce the periplasmatic DppA or the membrane
238 protein LysP.

239 In summary, the BtsS/BtsR and YpdA/YpdB sensing network helps *E. coli* to cope with
240 the additional metabolic burden imposed by protein overproduction.

241

242 **The BtsSR/YpdAB network limits the proportion of persister cells in wild-type**
243 **populations.** We hypothesized that the heterogeneous distribution of the capacity for protein
244 overproduction among the *btsSRypdAB* mutant population might be related to the presence of a
245 sub-population of cells that are unable to sense nutrient limitation and consequently fail to
246 activate transporters to acquire needed resources. Persister cells survive exposure to antibiotics
247 owing to their altered metabolic activity and low growth rate, but can subsequently resume
248 growth to form an antibiotic-sensitive population (20). We were interested to know whether the
249 BtsS/BtsR and YpdA/YpdB network has an influence on persister cell formation. To address this
250 question, we performed population-based studies by exposing growing WT or *btsSRypdAB*
251 mutant cells to ampicillin and determining the number of CFUs. Only cells able to recover from
252 the stress will form CFUs. We subdivided a growing culture and exposed cells to ampicillin
253 before and after the natural activation of the signaling systems, namely at OD_{600} of 0.4
254 (exponential growth phase) and 1.2 (post-exponential growth phase) (9). After treatment with
255 ampicillin a biphasic time-dependent killing curve was observed, which is typical for persister
256 formation (**Fig. 7**) (20). When cells were exposed to ampicillin prior to activation of the signaling
257 systems, the two strains exhibited almost identical patterns of response, characterized by a steep
258 initial decrease in CFUs followed by a slower killing rate, revealing persister cells (**Fig. 7A**).
259 Ampicillin treatment of cells after activation of the signaling systems resulted in a considerably
260 higher level of persister cells in the mutant (2.15%) than the WT (0.14%) population (**Fig. 7B**).

Accepted Manuscript Posted Online

Journal of Bacteriology

JB

Journal of Bacteriology

Downloaded from http://jb.asm.org/ on October 20, 2017 by UC London Library Services

In parallel, the minimum time taken to kill 99% of the population (MDK_{99}) (21) was determined for both strains after exposure to ofloxacin. The value for WT was determined to be 0.49 h and for the *btsSRypdAB* mutant 1.98 h, which is compatible with the higher fraction of persisters in the mutant population (**Fig. S2**).

These results reveal a novel role for the BtsS/BtsR and YpdA/YpdB signaling network in reducing the percentage of persister cells in a growing population. They are also in accordance with the idea of a contribution of both systems to help individual cells to replenish nutrient resources.

DISCUSSION

BtsS/BtsR (formerly YehU/YehT) is one of the most widespread TCSs in bacteria and is found in many human and plant pathogens. While most γ-proteobacteria contain this system, some, including *Escherichia*, *Citrobacter* and *Serratia*, have a second homologous system – YpdA/YpdB (22). Both belong to the LytS/LytTR-family. Previous systematic studies failed to identify a function for these TCSs (23, 24). We have now identified the HK BtsS as a high-affinity pyruvate receptor (K_d 58.6 µM), and YpdA/YpdB as a system that responds to higher levels (> 0.6 mM) of the same compound (8, 10). The target genes regulated by the two systems code for the high-affinity pyruvate/H^+ symporter YjiY [recently renamed BtsT (12)], and a transporter of unknown function, YhjX. However, the biological significance of the BtsS/BtsR and YpdA/YpdB systems has remained unclear.

Therefore, we first investigated the activation of the target genes of each system at the single-cell level using promoter fusions. We found that in clonal populations carrying chromosomally integrated copies of either P_{yjiY}-*gfp* or P_{yhjX}-*gfp* were heterogeneously activated when grown in LB medium, which is rich in amino acids (**Fig. 2**), and that induction of P_{yjiY}-*gfp*

Accepted Manuscript Posted Online

Journal of Bacteriology

JB

Journal of Bacteriology

Downloaded from http://jb.asm.org/ on October 20, 2017 by UC London Library Services

was slightly more variable than that of P_{yhjX}-*gfp*. In both cases, a predominantly unimodal Gaussian distribution of activation levels was observed, and only a very small percentage of cells remained in the OFF state. This pattern of activation differs markedly from the "all-or-nothing", switch-like gene expression described for the *lac* or *ara* promoter (25, 26). However, the heterogeneous, but unimodal activation of *yhjX* and *yjiY* can, in principle, be explained by the multiple factors known to affect their expression: (i) binding of the respective transcriptional activators BtsR and YdpB (27), (ii) the influence of the cAMP/CRP protein (P_{yjiY}), (iii) fine-tuning by the carbon starvation regulator CsrA (**Fig. 1**), and (iv) variations in the physiological state between cells (see below).

YpdA/YpdB-mediated activation of P_{yhjX} was found to be dependent on the concentration of pyruvate in the medium, and became homogenous when cells were grown in minimal medium containing pyruvate (20 mM) as the sole carbon source (**Fig. 3**). In contrast, under all tested conditions BtsS/BtsR-mediated activation of P_{yjiY} was characterized by high cell-to-cell variability, which was virtually unaffected by the amount of pyruvate in the medium (**Fig. 4**). It is important to note that the BtsS/BtsR systems, whose target gene codes for a high-affinity pyruvate transporter, is only activated by external pyruvate when cells concurrently face nutrient limitation (**Fig. 4** and (10)). The high degree of heterogeneity might reflect variations in the nutritional state of individual cells and differing needs for the high-affinity pyruvate transporter YjiY. Therefore, the BtsS/BtsR system responds only when cells are in need of a high-affinity uptake transporter to scavenge traces of available nutrients, e.g. pyruvate.

It has been proposed that cellular metabolism is both inherently stochastic and a generic source of phenotypic heterogeneity (28). In this general context, the results of our single-cell studies can be accommodated by the following model for the role of the two LytS/LytTR-type systems in *E. coli*. Under certain conditions, e.g. during growth in LB medium, cells excrete

Accepted Manuscript Posted Online

Journal of Bacteriology

JB

Journal of Bacteriology

Downloaded from http://jb.asm.org/ on October 20, 2017 by UC London Library Services

pyruvate due to overflow metabolism. Subsequently, other nutrients are depleted and cells sense the availability of pyruvate. Depending on the external pyruvate concentration and their particular nutritional needs, individual *E. coli* cells activate either the high-affinity BtsS/BtsR and/or the low-affinity YpdA/YpdB system upon entry into the post-exponential growth phase. The interplay between transporters with different affinities for the same substrate has already been described, and seems to be a successful strategy under nutrient limitation (29).

By using a reporter for the rate of ribosome synthesis, we found that only populations of reporter cells harboring the nutrient-sensing network exhibited unimodal activation of the *rrn*B P1 promoter, whereas the *btsSRypdAB* mutant was characterized by a bimodal expression pattern (**Fig. 5**). The heterogeneous activation of either P_{yjiY} or P_{yhjX} in individual WT cells allows uptake of nutrients, e.g. pyruvate, according to the individual requirement of the cells. This results in a unimodal distribution of the activation level of the *rrnB* P1 promoter characteristic of growing cells. It should be noted, that previous physiological studies revealed that *E. coli* has more than one pyruvate transporter (30), although only YjiY has thus far been characterized as high affinity pyruvate transporter (12). Therefore, we assume that individuals within the population of the *btsSRypdAB* mutant can cope with the lack of the sensing/transport of pyruvate and have normal ribosome synthesis. In addition, we imposed a metabolic burden by forcing cells to overproduce particular proteins. This is a natural scenario, as many pathogens have to produce virulence factors, exoenzymes, siderophores etc. in large amounts. While all WT cells managed to cope with this burden, about 50 % of cells of the mutant failed to overproduce the test protein GFP, a pattern which we also observed for the activation of the *rrnB* P1 promoter (**Fig. 6**). It should be noted that the evolved *E. coli* C41 (DE3) strain, which has been optimized for protein overproduction, has a point mutation in *btsS* that leads to stimulus-independent expression of *yjiY* (18). In light with the results presented here, the constitutive expression of the high-affinity

Accepted Manuscript Posted Online

pyruvate transporter YjiY (BtsT) in strain C41 guarantees a sufficient uptake of pyruvate in all cells independent from external or internal factors. Finally, a population-based persister assay revealed that *btsSRypdAB* populations contain a higher percentage of antibiotic-tolerant persister cells (dormant cells) than do WT populations (**Fig. 7**).

Taking these results into account, the model described above can be further extended. Sensing of external pyruvate by the BtsS/BtsR and YpdA/YpdB systems and the tight regulation of expression of the two transporters YjiY and YhjX depending on the needs of the individual cell ensures an optimization of the physiological state within the whole population to withstand upcoming metabolic stress. These findings are important in light of the host colonization of pathogenic species and their persistence, but also for metabolic engineering.

Downloaded from http://jb.asm.org/ on October 20, 2017 by UC London Library Services

Journal of Bacteriology JB Journal of Bacteriology

Accepted Manuscript Posted Online

Journal of Bacteriology

JB

Journal of Bacteriology

Downloaded from http://jb.asm.org/ on October 20, 2017 by UC London Library Services

345 **MATERIALS AND METHODS**

346 **Bacterial strains and growth conditions**. *E. coli* strains, their genotypes and plasmids
347 used in this study are listed in **Table 1**. Mutants were constructed using an *E. coli* Quick-and-
348 Easy gene deletion kit (Gene Bridges) and a BAC modification kit (Gene Bridges), as previously
349 reported (31). Both kits rely on the Red/ET recombination technique. Oligonucleotide sequences
350 are available on request.

351 *E. coli* MG1655 strains (**Table 1**) were grown overnight in lysogeny broth (LB) (10 g/l
352 NaCl, 10 g/l tryptone, 5 g/l yeast extract). After inoculation, bacteria were routinely grown in LB
353 medium under agitation (200 rpm) at 37°C. For solid medium, 1.5% (wt/vol) agar was added.
354 Where appropriate, media were supplemented with antibiotics (kanamycin sulfate, 50 µg/ml;
355 ampicillin sodium salt, 100 µg/ml). For the "low-nutrient environment" experiments, cells from
356 an overnight culture in LB were inoculated into 0.1x diluted LB at a starting OD_{600} of 0.05, and
357 grown for 1 h. Pyruvate was then added to the cultures to a final concentration of 0.01, 0.05, 0.1,
358 0.2, 1 or 20 mM, respectively.

359 *E. coli* MG1655 strains were also grown overnight in M9 minimal medium with 0.5%
360 (wt/vol) glucose as sole carbon source. Bacteria were then inoculated into M9 minimal medium
361 supplemented with increasing concentrations of pyruvate (0.3, 0.6, 1, 2 and 10 mM), and the total
362 carbon source concentration was adjusted to 20 mM using succinate. The conjugation strain *E.*
363 *coli* ST18 was grown in the presence of 50 µg/ml 5-aminolevulinic acid (ALA).

364

365 **Construction of fluorescence reporters**. Molecular manipulations were carried out
366 according to standard protocols (32). Plasmid DNA and genomic DNA were isolated using a
367 HiYield plasmid mini-kit (Sued-Laborbedarf) and a DNeasy blood and tissue kit (Qiagen),
368 respectively. DNA fragments were purified from agarose gels using a HiYield PCR cleanup and

Accepted Manuscript Posted Online

Journal of Bacteriology

JB

Journal of Bacteriology

Downloaded from http://jb.asm.org/ on October 20, 2017 by UC London Library Services

369 gel extraction kit (Sued-Laborbedarf). Q5 DNA polymerase (New England BioLabs) was used
370 according to the supplier's instructions. Restriction enzymes and other DNA-modifying enzymes
371 were also purchased from New England BioLabs and used according to the manufacturer's
372 directions. Replicative plasmids were transferred into *E. coli* strains using competent cells
373 prepared as described in (33).

374 For construction of the promoter-*gfp* fusions, 300-bp segments of the region immediately
375 upstream of the coding sequence were amplified using oligonucleotide pairs containing
376 EcoRI/PspOMI restriction sites. The resulting promoter fragments were ligated into the γ-origin-
377 dependent vector pNPTS138-R6KT-*gfp* after restriction with EcoRI/PspOMI. Chromosomal
378 insertions of promoter-*gfp* into the designated *E. coli* strains were achieved by integrating the
379 resultant suicide vectors pNPTS138-R6KT-P_{yhjX}-*gfp* and pNPTS138-R6KT-P_{yjiY}-*gfp* via RecA-
380 mediated single homologous recombination as described previously (13). The donor strain *E. coli*
381 ST18, containing the required plasmids, was cultivated together with the recipient *E. coli*
382 MG1655 strain in LB medium, supplemented with additives as described, to an OD_{600} of about
383 0.8. Recombination-positive clones were selected on kanamycin plates, and correct chromosomal
384 integration was checked by PCR and sequencing. To prevent duplication instability, the reporter
385 strains were always cultivated in the presence of kanamycin.

386

387 **Single-cell fluorescence microscopy and analysis.** To measure promoter activity in
388 individual cells of the reporter strains, cells were cultivated as described above in a rotary shaker.
389 Samples were taken (10 µL) and analyzed on an agarose pad [0.5% (wt/vol) agarose in PBS
390 buffer, pH 7.4], which was placed on a microscope slide and covered with a coverslip.

391 Images were taken on a Leica microscope (DMI 6000B) equipped with a Leica DFC 365
392 Fx camera (Andor, 12bit). An excitation wavelength of 460 nm and a 512 nm emission filter with

Accepted Manuscript Posted Online

Journal of Bacteriology

JB

Journal of Bacteriology

Downloaded from http://jb.asm.org/ on October 20, 2017 by UC London Library Services

393 a 75-nm bandwidth were used for visualization of GFP fluorescence and an excitation
394 wavelength of 546 nm and a 605 nm emission filter with the same bandwidth were used for
395 visualization of red fluorescence. A minimum of 200 cells per condition was analyzed. The
396 digital images were analyzed using Fiji (34) and statistical analysis was performed using
397 GraphPad Prism version 5.03 for Windows (GraphPad Software, La Jolla California USA,
398 www.graphpad.com). The background fluorescence was subtracted from each field of view.
399 The noise was calculated by dividing the standard deviation by the mean. The higher the
400 noise value the more heterogeneous the distribution. The percentage of dark cells was determined
401 from the number of cells whose fluorescence levels overlapped with the negative control (before
402 activation) and the total number of cells quantified. The frequency distributions depict the
403 fraction of values which lie within the range of values that define the bin. The bin range was kept
404 constant at 20 AU. Propidium iodide (Invitrogen, Oregon) was added to the cell cultures at a final
405 concentration of 5 µM to stain dead cells (red fluorescence).
406
407
408 **Overproduction experiments**. Overnight cultures of *E. coli* MG1655 transformed with
409 the plasmid pBAD24-*gfp* were diluted 100-fold in 20 ml of fresh LB medium supplemented with
410 100 µg/ml of ampicillin sodium salt and incubated aerobically at 37 °C until OD_{600} reached 0.6
411 (early exponential phase). Cells were induced with L-arabinose 0.2% (wt/vol) for 1 h. Before and
412 after induction, 100-µl samples were taken, diluted 1:1,000 in PBS and analyzed in a BD
413 Accuri™ C6 flow cytometer equipped with a solid-state laser (488 nm-emission; 20 mW). The
414 green fluorescence emission from GFP was collected by the FL1 filter (BP 533/30 filter).
415 Forward-angle light scatter (FSC) and side-angle light scatter (SSC) were collected in the FSC
416 detector and SSC filter (BP 488/10 filter), respectively. The detection threshold was adjusted for

Accepted Manuscript Posted Online

Journal of Bacteriology

JB

FSC to eliminate noise, and the gate was set on the FSC-SSC dot plot to exclude debris. Sheath flow rate was 14 µl/min and no more than 100 events/second were acquired. For each sample run, a maximum of 2,000 events were collected. Analysis of data was carried out using Cytospec software (http://www.cyto.purdue.edu/Purdue_software)

Persister cell assay. To determine the number of persister cells, the number of colony-forming units (CFUs) per ml was measured following exposure of the culture to 200 µg/ml ampicillin. Overnight cultures were diluted 100-fold in 20 ml of fresh LB medium and incubated aerobically at 37 °C until OD_{600} reached 0.4 or 1.2. Aliquots were then transferred to a new 100-ml flask (final OD_{600} =1) and the antibiotic was added. Every hour during antibiotic treatment, samples were taken, serially diluted in PBS, plated on LB agar and incubated at 37°C for 16 h. CFUs were counted as a measure of surviving persister cells. Persisters were calculated as the surviving fraction by dividing the number of CFUs/ml in the culture after incubation with the antibiotic by the number of CFUs/ml in the culture before addition of the antibiotic. Each experiment was repeated on three different days.

For calculation of the minimum duration of killing (MDK_{99}), the procedure described above was performed using ofloxacin (at a final concentration of 5 µg/ml) as the antibiotic. The MDK_{99} value corresponds to the time (in hours) needed to kill 99% of the initial population.

Journal of Bacteriology

Downloaded from http://jb.asm.org/ on October 20, 2017 by UC London Library Services

Accepted Manuscript Posted Online

Acknowledgments

We thank Dr. Nicola Lorenz and Tobias Bauer for strain construction and Lena Stelzer for excellent technical assistance. We thank Prof. Dr. Regine Hengge and Dr. Gisela Klauck for providing plasmids. This work was financially supported by the Deutsche Forschungsgemeinschaft (DFG) SPP1617, projects JU270/13-2 (KJ) and KO 4537/1-2 (DK). The funders had no role in study, design, data collection and interpretation, or the decision to submit the work for publication.

Downloaded from http://jb.asm.org/ on October 20, 2017 by UC London Library Services

Journal of Bacteriology JB Journal of Bacteriology

Accepted Manuscript Posted Online

Journal of Bacteriology

JB

Journal of Bacteriology

Downloaded from http://jb.asm.org/ on October 20, 2017 by UC London Library Services

446 **REFERENCES**

447 1. **Mascher T**, **Helmann JD**, **Unden G**. 2006. Stimulus perception in bacterial signal-
448 transducing histidine kinases. Microbiol Mol Biol Rev **70**:910–938.

449 2. **Stock AM**, **Robinson VL**, **Goudreau PN**. 2000. Two-component signal transduction.
450 Annu Rev Biochem **69**:183–215.

451 3. **Sidote DJ**, **Barbieri CM**, **Wu T**, **Stock AM**. 2008. Structure of the *Staphylococcus*
452 *aureus* AgrA LytTR Domain Bound to DNA Reveals a Beta Fold with an Unusual Mode
453 of Binding. Structure **16**:727–735.

454 4. **Qin X**, **Singh K V.**, **Weinstock GM**, **Murray BE**. 2000. Effects of *Enterococcus faecalis*
455 fsr genes on production of gelatinase and a serine protease and virulence. Infect Immun
456 **68**:2579–2586.

457 5. **Shimizu T**, **Shima K**, **Yoshino K**, **Yonezawa K**, **Shimizu T**, **Hayashi H**. 2002. Proteome
458 and Transcriptome Analysis of the Virulence Genes Regulated by the VirR / VirS System
459 in *Clostridium perfringens* **184**:2587–2594.

460 6. **Rood JI**. 1998. Virulence genes of *Clostridium perfringens*. Annu Rev Microbiol **52**:333–
461 360.

462 7. **Kraxenberger T**, **Fried L**, **Behr S**, **Jung K**. 2012. First insights into the unexplored two-
463 component system YehU/YehT in *Escherichia coli*. J Bacteriol **194**:4272–84.

464 8. **Fried L**, **Behr S**, **Jung K**. 2013. Identification of a target gene and activating stimulus for
465 the YpdA/YpdB histidine kinase/response regulator system in *Escherichia coli*. J Bacteriol
466 **195**:807–15.

467 9. **Behr S**, **Fried L**, **Jung K**. 2014. Identification of a novel nutrient-sensing histidine
468 kinase/response regulator network in *Escherichia coli*. J Bacteriol **196**:2023–9.

469 10. **Behr S**, **Kristoficova I**, **Witting M**, **Breland EJ**, **Eberly AR**, **Sachs C**, **Schmitt-Kopplin**
470 **P**, **Hadjifrangiskou M**, **Jung K**. 2017. Identification of a High-Affinity Pyruvate
471 Receptor in *Escherichia coli*. Sci Rep **7**:1388.

472 11. **Pao SS**, **Paulsen IT**, **Saier MH**. 1998. Major Facilitator Superfamily. Microbiol Mol Biol
473 Rev **62**:1–34.

474 12. **Kristoficova I**, **Vilhena C**, **Behr S**, **Jung K**. BtsT - a novel and specific pyruvate/H+
475 symporter in *Escherichia coli*. Submitted for publication.

476 13. **Fried L**, **Lassak J**, **Jung K**. 2012. A comprehensive toolbox for the rapid construction of
477 lacZ fusion reporters. J Microbiol Methods **91**:537–543.

478 14. **Shah D**, **Zhang Z**, **Khodursky A**, **Kaldalu N**, **Kurg K**, **Lewis K**. 2006. Persisters: a
479 distinct physiological state of *E. coli*. BMC Microbiol **6**:53.

480 15. **Bartlett MS**, **Gourse RL**. 1994. Growth rate-dependent control of the *rrnB* P1 core
481 promoter in *Escherichia coli*. J Bacteriol **176**:5560–5564.

Accepted Manuscript Posted Online

16. **Shan Y**, **Gandt AB**, **Rowe SE**, **Deisinger JP**, **Conlon BP**, **Lewis K**. 2017. ATP-Dependent Persister Formation in *Escherichia coli*. mBio **8**:1–14.

17. **Miroux B**, **Walker JE**. 1996. Over-production of Proteins in *Escherichia coli* : Mutant Hosts that Allow Synthesis of some Membrane Proteins and Globular Proteins at High Levels. J Mol Bio 289–298.

18. **Schlegel S**, **Genevaux P**, **de Gier JW**. 2015. De-convoluting the Genetic Adaptations of *E.coli* C41(DE3) in Real Time Reveals How Alleviating Protein Production Stress Improves Yields. Cell Rep **10**:1758–1766.

19. **Santini CL**, **Bernadac A**, **Zhang M**, **Chanal A**, **Ize B**, **Blanco C**, **Wu LF**. 2001. Translocation of Jellyfish Green Fluorescent Protein via the Tat System of *Escherichia coli* and Change of Its Periplasmic Localization in Response to Osmotic Up-shock. J Biol Chem **276**:8159–8164.

20. **Lewis K**. 2010. Persister cells. Annu Rev Microbiol **64**:357–372.

21. **Brauner A**, **Fridman O**, **Gefen O**, **Balaban NQ**. 2016. Distinguishing between resistance, tolerance and persistence to antibiotic treatment. Nat Publ Gr **14**:320–330.

22. **Behr S**, **Brameyer S**, **Witting M**, **Schmitt-Kopplin P**, **Jung K**. 2017. Comparative analysis of LytS/LytTR-type histidine kinase/response regulator systems in γ-proteobacteria. PLoS One **12**:e0182993.

23. **Oshima T**, **Aiba H**, **Masuda Y**, **Kanaya S**, **Sugiura M**, **Wanner BL**, **Mori H**, **Mizuno T**. 2002. Transcriptome analysis of all two-component regulatory system mutants of *Escherichia coli* K-12. Mol Microbiol **46**:281–291.

24. **Zhou L**, **Lei X-H**, **Bochner BR**, **Wanner BL**. 2003. Phenotype MicroArray Analysis of *Escherichia coli* K-12 Mutants with Deletions of All Two-Component Systems. J Bacteriol **185**:4956–4972.

25. **Ozbudak EM**, **Thattai M**, **Lim HN**, **Shraiman BI**, **Van Oudenaarden A**. 2004. Multistability in the lactose utilization network of *Escherichia coli*. Nature **427**:737–740.

26. **Megerle JA**, **Fritz G**, **Gerland U**, **Jung K**, **Rädler JO**. 2008. Timing and Dynamics of Single Cell Gene Expression in the Arabinose Utilization System. Biophys J **95**:2103–2115.

27. **Behr S**, **Heermann R**, **Jung K**. 2016. Insights into the DNA-binding mechanism of a LytTR-type transcription regulator. Biosci Rep **36**:e00326.

28. **Kiviet DJ**, **Nghe P**, **Walker N**, **Boulineau S**, **Sunderlikova V**, **Tans SJ**. 2014. Stochasticity of metabolism and growth at the single-cell level. Nature **514**:376–379.

29. **Levy S**, **Kafri M**, **Carmi M**, **Barkai N**. 2011. The competitive advantage of a dual-transporter system. Science **334**:1408–1412.

30. **Kreth J**, **Lengeler JW**, **Jahreis K**. 2013. Characterization of Pyruvate Uptake in *Escherichia coli* K-12. PLoS One **8**:6–12.

Journal of Bacteriology

JB

Journal of Bacteriology

Downloaded from http://jb.asm.org/ on October 20, 2017 by UC London Library Services

Accepted Manuscript Posted Online

31. **Heermann R**, **Zeppenfeld T**, **Jung K**. 2008. Simple generation of site-directed point mutations in the Escherichia coli chromosome using Red(R)/ET(R) Recombination. Microb Cell Fact **7**:14.

32. **Sambrook J**, **Fritsch EF**, **Maniatis T**. 1989. Molecular Cloning: A Laboratory Manual. Cold Spring Harbor laboratory press. New York.

33. **Inoue H**, **Nojima H**, **Okayama H**. 1990. High efficiency transformation of *Escherichia coli* with plasmids. Gene **96**:23–28.

34. **Schindelin J**, **Arganda-Carreras I**, **Frise E**, **Kaynig V**, **Longair M**, **Pietzsch T**, **Preibisch S**, **Rueden C**, **Saalfeld S**, **Schmid B**, **Tinevez J-Y**, **White DJ**, **Hartenstein V**, **Eliceiri K**, **Tomancak P**, **Cardona A**. 2012. Fiji: an open-source platform for biological-image analysis. Nat Methods **9**:676–82.

35. **Blattner FR**, **Plunkett G**, **Bloch CA**, **Perna NT**, **Burland V**, **Riley M**, **Collado-Vides J**, **Glasner JD**, **Rode CK**, **Mayhew GF**, **Gregor J**, **Davis NW**, **Kirkpatrick HA**, **Goeden MA**, **Rose DJ**, **Mau B**, **Shao Y**. 1997. The Complete Genome Sequence of *Escherichia coli* K-12. Science (80-) **277**:1453–1462.

36. **Thoma S**, **Schobert M**. 2009. An improved *Escherichia coli* donor strain for diparental mating. FEMS Microbiol Lett **294**:127–132.

37. **Taylor RG**, **Walker DC**, **McInnes RR**. 1993. *E. coli* host strains significantly affect the quality of small scale plasmid DNA preparations used for sequencing. Nucleic Acids Res **21**:1677–1678.

38. **Cherepanov PP**, **Wackernagel W**. 1995. Gene disruption in *Escherichia coli*: TcR and KmR cassettes with the option of Flp-catalyzed excision of the antibiotic-resistance determinant. Gene **158**:9–14.

39. **Guzman LM**, **Belin D**, **Carson MJ**, **Beckwith J**. 1995. Tight regulation, modulation, and high-level expression by vectors containing the arabinose pBAD promoter. J Bacteriol **177**:4121–4130.

40. **Tetsch L**, **Koller C**, **Haneburger I**, **Jung K**. 2008. The membrane-integrated transcriptional activator CadC of *Escherichia coli* senses lysine indirectly via the interaction with the lysine permease LysP. Mol Microbiol **67**:570–583.

Downloaded from http://jb.asm.org/ on October 20, 2017 by UC London Library Services

Journal of Bacteriology JB Journal of Bacteriology

Accepted Manuscript Posted Online

TABLE 1- Bacterial strains and plasmids used in this study.

Strains and plasmids	Relevant genotype or description	Reference or source
***E. coli* strains**		
MG1655	F^- λ^- *ilvG rfb50 rph-1*	(35)
ST18	S17lpir Δ*hemA*	(36)
DH5α	*fhuA2 lac*Δ*U169 phoA glnV44 Φ80' lacZ* Δ*M15 gyrA96 recA1 relA1 endA1 thi-1 hsdR17*$^-$	(37)
MG 35	MG1655 Δ*btsSbtsR* Δ*ypdAypdB*	This work
MG 2	MG1655 Δ*yehUT* = Δ*btsSR*	(7)
MG 20	MG1655 Δ*ypdAB*	(8)
MG1655 P_{yhjX}-*gfp*	Integration of P_{yhjX}-*gfp* at the native locus in *E. coli* MG1655	This work
MG1655 P_{yjiY}-*gfp*	Integration of P_{yjiY}-*gfp* at the native locus in *E. coli* MG1655	This work
MG1655 $P_{rrnB\ P1}$-*gfp*	Integration of $P_{rrnB\ P1}$-*gfp* at the native locus in *E. coli* MG1655	This work
MG1655 35 $P_{rrnB\ P1}$-*gfp*	Integration of $P_{rrnB\ P1}$-*gfp* at the native locus in *E. coli* MG 35	This work
Plasmids		
pRed/ET	λ-RED recombinase in pBAD24, Amp^r	Gene Bridges
pCP20	FLP-recombinase, λcI 857^+, λpR Rep^{ts}, Amp^r, Cm^r	(38)
pNPTS138-R6KT	*mobRP4*$^+$ *ori*-R6K *sacB*, suicide plasmid, Kan^r	(13)
pNPTS138-R6KT-P_{yhjX}-*gfp*	300 bp of P_{yhjX} fused to *gfp* and cloned into EcoRI/PspOMI sites of pNPTS138-R6KT; Kan^r	This work

Journal of Bacteriology
JB
Journal of Bacteriology
Downloaded from http://jb.asm.org/ on October 20, 2017 by UC London Library Services

Accepted Manuscript Posted Online

pNPTS138-R6KT-P_{yjiY}-*gfp*	300 bp of P_{yjiY} fused to *gfp* and cloned into EcoRI/PspOMI sites of pNPTS138-R6KT; Kan^r	This work
pNPTS138-R6KT-$P_{rrnB\ P1}$-*gfp*	300 bp of $P_{rrnB\ P1}$ fused to *gfp* and cloned into EcoRI/PspOMI sites of pNPTS138-R6KT; Kan^r	This work
pXGSF	*gfp* under the control of a vegetative synthetic promoter	G. Klauck and R. Hengge, unpublished
pBAD24	Arabinose-inducible P_{BAD} promoter, pBR322 ori; Amp^r	(39)
pBAD24-*gfp*	*gfp* cloned in the EcoRI and NcoI sites of pBAD24	(26)
pBAD24-RR-*gfp*	*gfp-mut2* cloned in the NheI and HindIII sites of p8754, derivative of pBAD24	(19)
pBAD24-RR-*gfpmut-dppA*	*dppA* cloned in the HindIII site of pBAD24- RR-*gfpmut2* Expression vector, ColA ori, Kan^r	This work
pCOLA Duet-1	*gfp* under the control of the IPTG-inducible *lac* promoter cloned in	Merck (Darmstadt)
pCOLA-P_{lac}-*gfp*	the BamHI and HindIII of pCOLA-Duet-1	This work
	lysP in pBAD33, Cm^r	
pBAD33-*lysP*	*mcherry* cloned in the NcoI pBAD33-*lysP*, Cm^r	(40)
pBAD33-*lysP-mcherry*		This work

550

Downloaded from http://jb.asm.org/ on October 20, 2017 by UC London Library Services

Journal of Bacteriology JB Journal of Bacteriology

Accepted Manuscript Posted Online

Journal of Bacteriology

JB

Journal of Bacteriology

Downloaded from http://jb.asm.org/ on October 20, 2017 by UC London Library Services

551 **FIGURE LEGENDS**

552

553 **FIG 1** Model of the nutrient-sensing BtsS/BtsR and YpdA/YpdB network in *E. coli*. The scheme
554 summarizes the signal transduction cascades triggered by the BtsS/BtsR and YpdA/YpdB
555 systems and the influence of other regulatory elements. Activating (→) and inhibitory (⊦) effects
556 are indicated. PP, periplasm; CM, cytoplasmic membrane; CP, cytoplasm. See text for details.

557 **FIG 2** Single-cell analysis of P_{yhjX} and P_{yjiY} activation during growth in LB medium. *E. coli* cells
558 expressing *gfp* under the control of the *yhjX* or *yjiY* promoter, respectively, were grown in LB
559 medium, and fluorescence micrographs were taken before (exponential growth phase) and after
560 activation (post-exponential growth phase) of the two TCSs. Representative fluorescence and
561 phase-contrast images of P_{yhjX}-*gfp* and P_{yjiY}-*gfp* reporter strains are shown in panels **A** and **C**
562 respectively. The corresponding distributions of the fluorescence intensity of the P_{yhjX}-*gfp* and
563 P_{yjiY}-*gfp* reporter strains are depicted in panels **B** and **D**. Unfilled bars refer to values prior to
564 activation and filled bars to those observed after activation. Dashed lines represent the threshold
565 of activation for each of the reporter strains. A total of 200 cells was analyzed in each experiment
566 and frequency refers to the percentage of cells with the indicated intensity (see Materials and
567 Methods for details). The continuous curves represent Gaussian fits based on the histograms of
568 the fluorescence intensity. PH, phase contrast; AU, arbitrary units. Scale bar = 2 µm. Experiments
569 were performed independently three times.

570 **FIG 3** Effects of different external pyruvate concentrations on P_{yhjX}-*gfp* activation at the single-
571 cell level. *E. coli* cells expressing *gfp* under the control of the P_{yhjX} promoter were grown in M9
572 minimal medium containing increasing concentrations of pyruvate (supplemented with succinate,
573 final C-concentration 20 mM), and analyzed by fluorescence microscopy. A total of 200 cells

Accepted Manuscript Posted Online

Journal of Bacteriology

JB

Journal of Bacteriology

Downloaded from http://jb.asm.org/ on October 20, 2017 by UC London Library Services

574 was analyzed in each experiment at the time point of maximal expression and frequency refers to
575 the percentage of cells with the indicated intensity (see Materials and Methods). Histograms of
576 the fluorescence intensities of cells were fitted using a Gaussian distribution (solid line). The
577 dashed line represents the threshold of activation for the reporter strain. AU, arbitrary units.
578 Experiments were performed independently three times.

579 **FIG 4** Effects of different external pyruvate concentrations on P_{yjiY}-*gfp* activation at the single-
580 cell level. *E. coli* cells expressing *gfp* under the control of the P_{yjiY} promoter were grown in a
581 nutrient-poor environment (0.1x LB medium) for 1 h. The medium was then supplemented with
582 20 mM (**A**) or increasing pyruvate concentrations (**B**), and cells were subsequently analyzed by
583 fluorescence microscopy. A total of 200 cells were analyzed for each experiment and frequency
584 is represented as % of cells (refer to Material and Methods for detailed explanation). Histograms
585 of the fluorescence intensities of cells were fitted using a Gaussian distribution (solid line).
586 Dashed lines represent the threshold of activation for the reporter strain. AU, arbitrary units.
587 Experiments were performed three independent times. For further details, see the legends to Figs
588 2 and 3.

589 **FIG 5** In the absence of the BtsSR/YpdAB network, *rrnB* P1 promoter activity is low and
590 bistable. Wild-type (WT) *E. coli* MG1655 (blue) or mutant *btsSRypdAB* (red) cells harboring a
591 chromosomally encoded *rrnB* P1-*gfp* fusion were grown in LB medium and examined by
592 fluorescence microscopy. For further details, see the legends to Figs 2 and 3. A total of 200 cells
593 were analyzed for each experiment at the post-exponential growth phase and frequency is
594 represented as % of cells (refer to Material and Methods for detailed explanation). Histograms of
595 the fluorescence intensities of cells were fitted using a Gaussian distribution (solid line). AU,
596 arbitrary units. Experiments were performed three independent times.

Accepted Manuscript Posted Online

Journal of Bacteriology

JB

Journal of Bacteriology

Downloaded from http://jb.asm.org/ on October 20, 2017 by UC London Library Services

597

598 **FIG 6** The BtsSR/YpdAB network promotes homogenous protein overproduction in all cells.
599 Wild-type (WT) or *btsSRypdAB* mutant cells harboring the overproduction vector pBAD24-*gfp*
600 were grown in LB medium. Samples were taken before and after the addition of the inducer
601 arabinose [0.2 % (wt/vol)]. Cells were analyzed by fluorescence microscopy and flow cytometry.
602 Distributions of fluorescent cell counts and representative views of WT cells before and after
603 addition of arabinose are shown in panels **A** and **B**, while the corresponding data for the
604 *btsSRypdAB* mutant are depicted in panels **C** and **D**. About 2,000 events were recorded for each
605 plot. Cell counts represent numbers of cells and fluorescence intensity is given in arbitrary units
606 (AU). Scale bar = 2 μM. Experiments were performed independently three times.

607 **FIG 7** The BtsSR/YpdAB network reduces the proportion of persister cells in populations. Either
608 WT (blue lines) or mutant *btsSRypdAB* (red lines) cells were grown in LBmedium. Before
609 (exponential growth phase) (**A**) and after (**B**) activation (post-exponential growth phase) of the
610 systems, cells were exposed to ampicillin (200 μg/ml). Samples were taken and analyzed for
611 colony-forming units (CFUs). Three independent experiments were performed and error bars
612 indicate the standard deviations of the means.

613

614

Accepted Manuscript Posted Online

Journal of Bacteriology

JB

Journal of Bacteriology

FIG 1

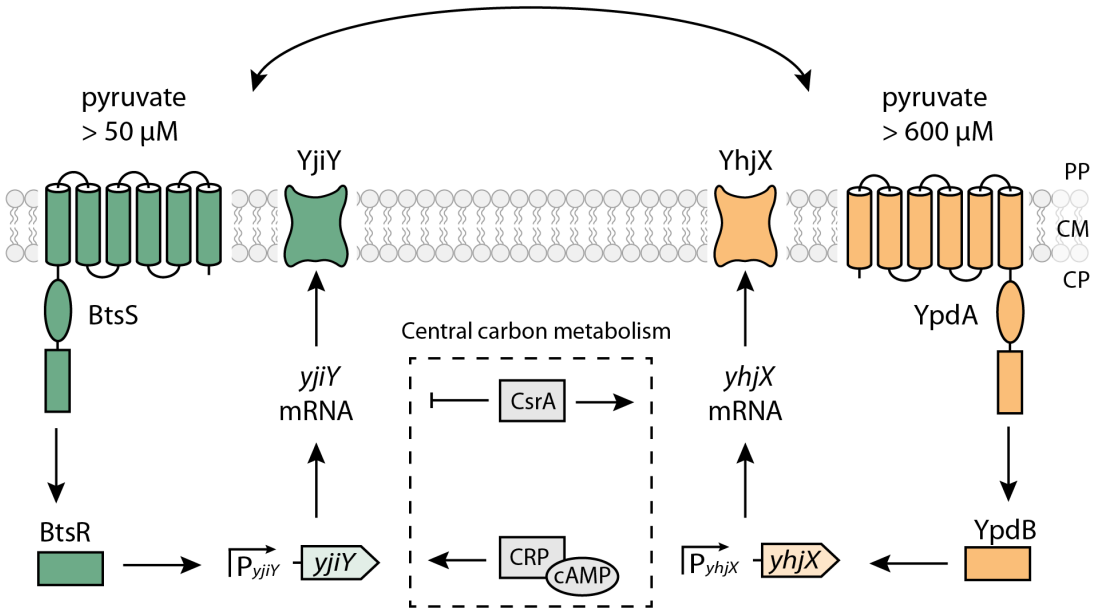

Downloaded from http://jb.asm.org/ on October 20, 2017 by UC London Library Services

Accepted Manuscript Posted Online

Journal of Bacteriology

JB

Journal of Bacteriology

FIG 2

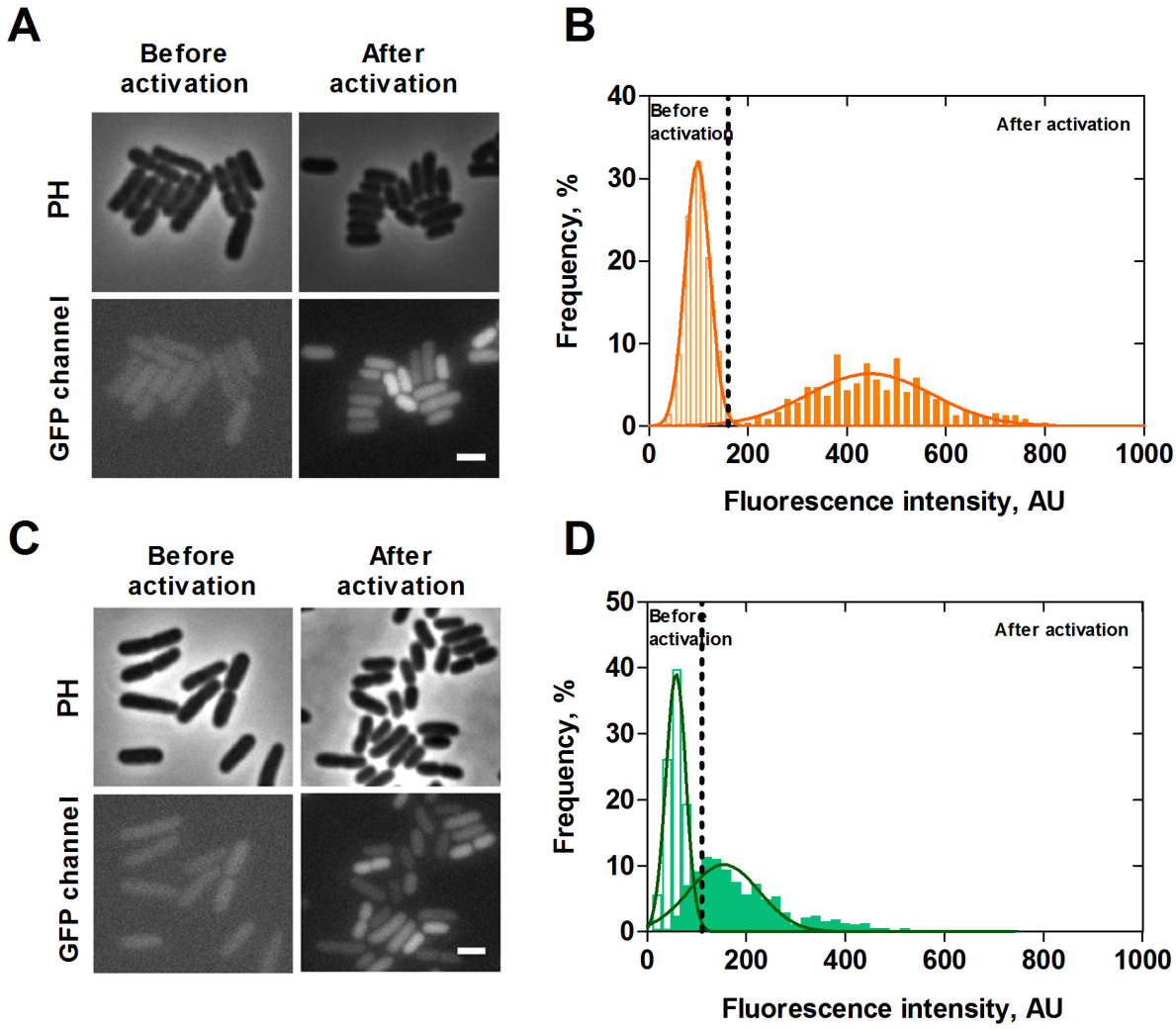

Downloaded from http://jb.asm.org/ on October 20, 2017 by UC London Library Services

Accepted Manuscript Posted Online
Journal of Bacteriology
JB
Journal of Bacteriology

FIG 3

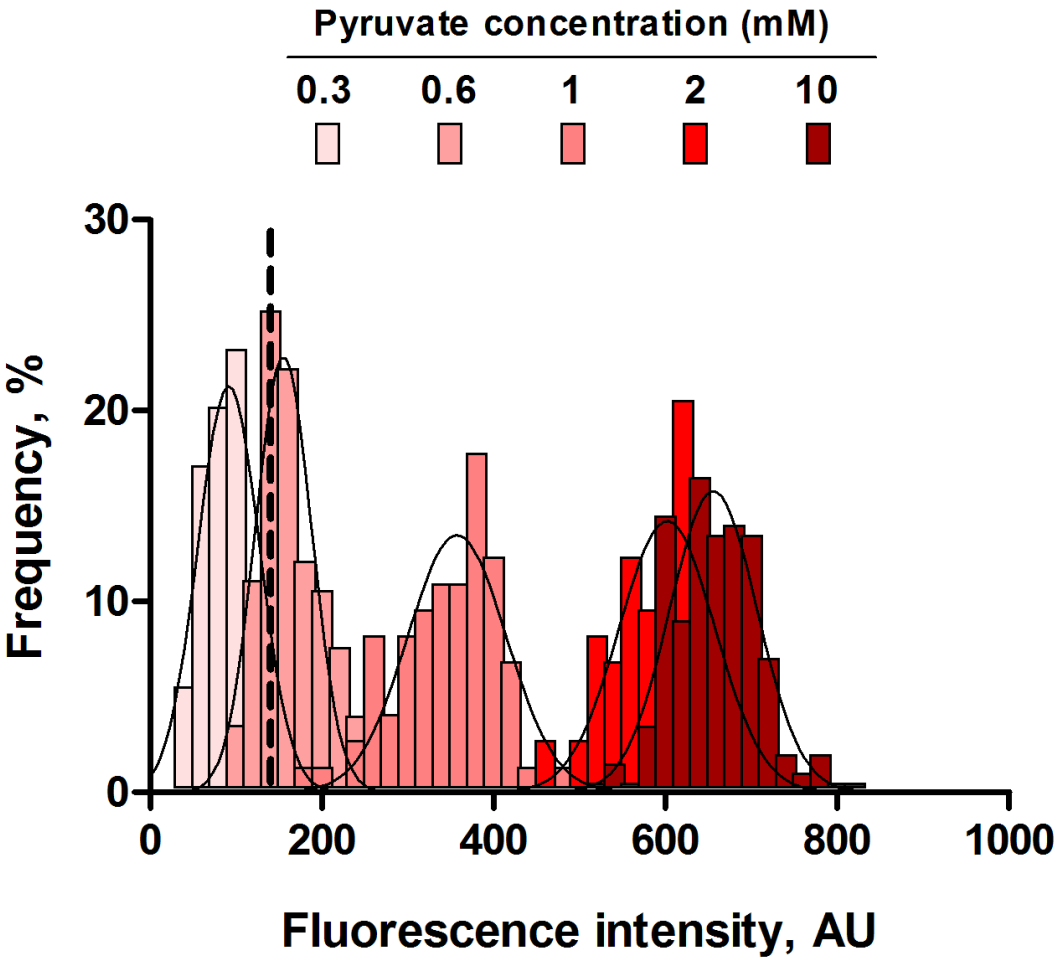

Downloaded from http://jb.asm.org/ on October 20, 2017 by UC London Library Services

Accepted Manuscript Posted Online

Journal of Bacteriology

JB

Journal of Bacteriology

FIG 4

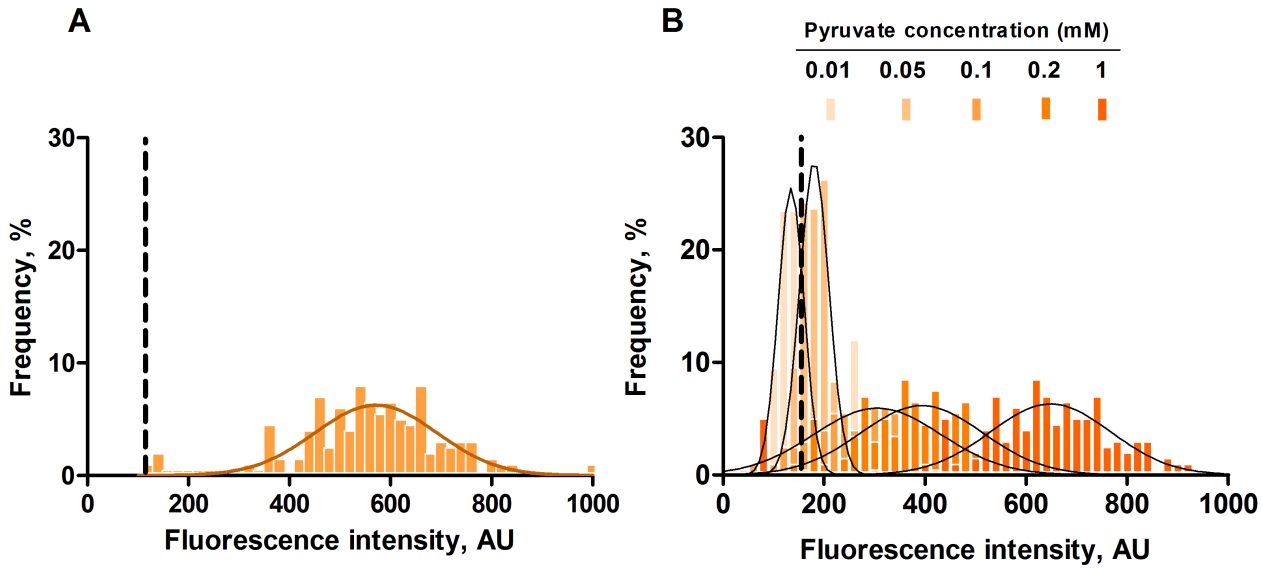

Downloaded from http://jb.asm.org/ on October 20, 2017 by UC London Library Services

Accepted Manuscript Posted Online

Journal of Bacteriology

JB

Journal of Bacteriology

FIG 5

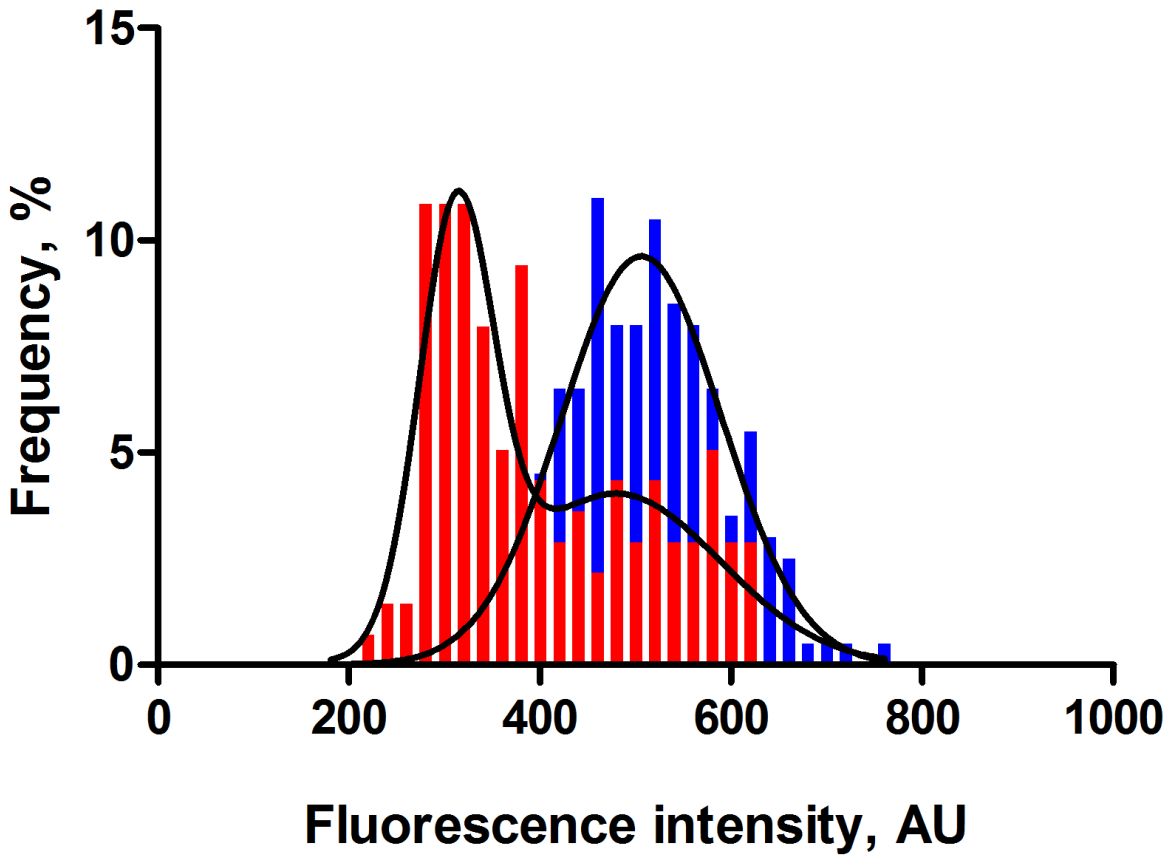

Downloaded from http://jb.asm.org/ on October 20, 2017 by UC London Library Services

Accepted Manuscript Posted Online
Journal of Bacteriology
JB
Journal of Bacteriology

FIG 6

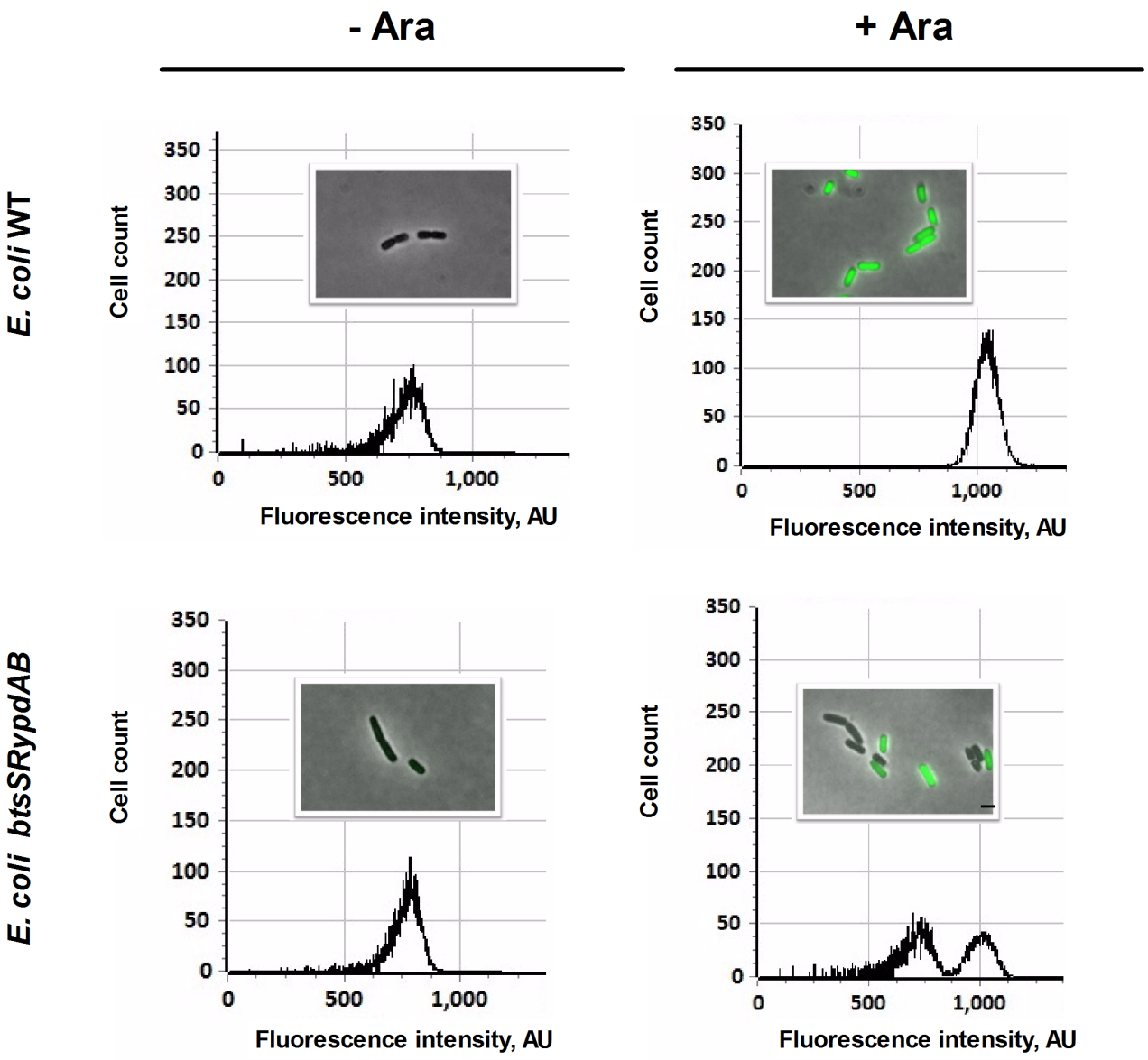

Downloaded from http://jb.asm.org/ on October 20, 2017 by UC London Library Services

Accepted Manuscript Posted Online

Journal of Bacteriology

JB

Journal of Bacteriology

FIG 7

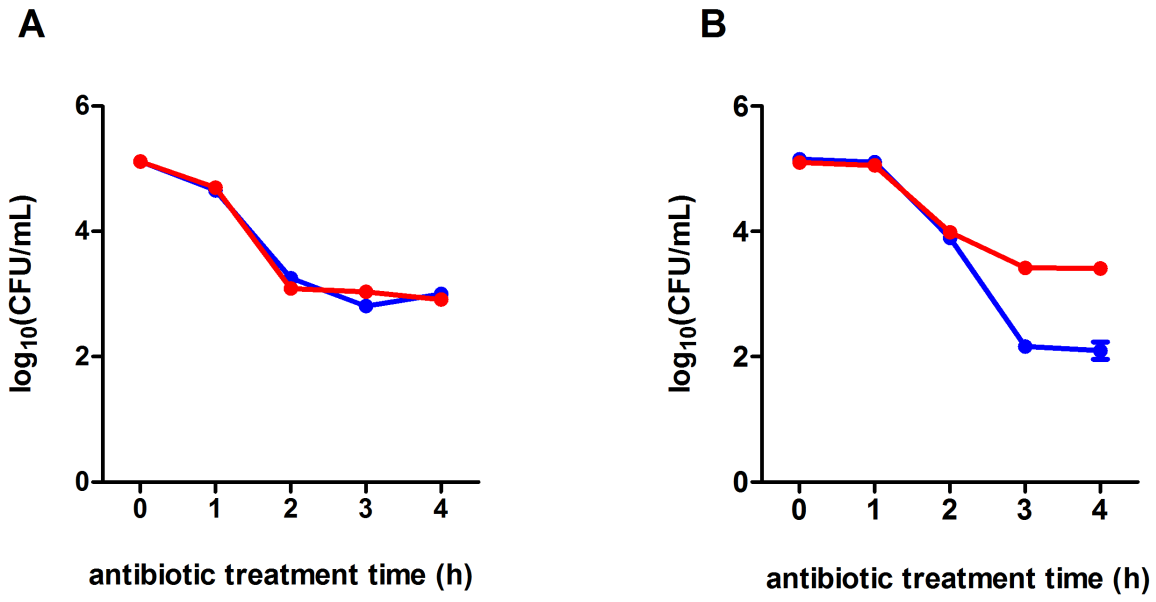

Downloaded from http://jb.asm.org/ on October 20, 2017 by UC London Library Services